



**HAL**  
open science

## Real-time optimization of the key filtration parameters in an AnMBR: Urban wastewater mono-digestion vs. co-digestion with domestic food waste

A Robles, Gabriel Capson-Tojo, M V Ruano, A Seco, J Ferrer

### ► To cite this version:

A Robles, Gabriel Capson-Tojo, M V Ruano, A Seco, J Ferrer. Real-time optimization of the key filtration parameters in an AnMBR: Urban wastewater mono-digestion vs. co-digestion with domestic food waste. *Waste Management*, 2018, 80, pp.299 - 309. 10.1016/j.wasman.2018.09.031 . hal-03777856

**HAL Id: hal-03777856**

**<https://hal.inrae.fr/hal-03777856v1>**

Submitted on 17 Aug 2023

**HAL** is a multi-disciplinary open access archive for the deposit and dissemination of scientific research documents, whether they are published or not. The documents may come from teaching and research institutions in France or abroad, or from public or private research centers.

L'archive ouverte pluridisciplinaire **HAL**, est destinée au dépôt et à la diffusion de documents scientifiques de niveau recherche, publiés ou non, émanant des établissements d'enseignement et de recherche français ou étrangers, des laboratoires publics ou privés.

Manuscript Number: WM-18-597

Title: Real-time optimization of the key filtration parameters in an AnMBR: urban wastewater mono-digestion vs. co-digestion with domestic food waste

Article Type: Full Length Article

Keywords: Anaerobic membrane bioreactor (AnMBR); process control; kitchen waste; fouling; modelling; urban wastewater

Corresponding Author: Dr. Àngel Robles, Ph.D.

Corresponding Author's Institution: Universitat de València

First Author: Àngel Robles, Ph.D.

Order of Authors: Àngel Robles, Ph.D.; Gabriel Capson-Tojo; María Victoria Ruano; Aurora Seco; José Ferrer

Abstract: This study describes a model-based method for real-time optimization of the key filtration parameters in a submerged anaerobic membrane bioreactor (AnMBR) treating urban wastewater (UWW) and UWW mixed with domestic food waste (FW). The method consists of three statistical analyses: (1) Morris screening method to identify the key filtration parameters; (2) Monte Carlo method to establish suitable initial control inputs values; and (3) optimization algorithm for minimizing the operating costs. The operating filtration cost after implementing the control methodology was €0.047 per m<sup>3</sup> (59.6% corresponding to energy costs) when treating UWW and €0.067 per m<sup>3</sup> when adding FW due to higher fouling rates. However, FW increased the biogas productivities, reducing the total costs to €0.035 per m<sup>3</sup>. Average downtimes for reversible fouling removal of 0.4% and 1.6% were obtained, respectively. The results confirm the capability of the proposed control system for optimizing the AnMBR performance when treating both substrates.

Suggested Reviewers: Ilse Smets  
Professor, Faculty of Engineering Science, KU Leuven  
ilse.smets@kuleuven.be  
Expertise on Anaerobic Membrane Bioreactors

Adam Smith  
Professor, Astani Department of Civil and Environmental Engineering,  
University of Southern California  
smithada@usc.edu  
Expertise on Anaerobic Membrane Bioreactors for food waste and urban  
wastewater treatment

Ignasi Rodríguez-Roda i Layret  
Professor, ENGINYERIA QUÍMICA, AGRÀRIA I TECNOLOGIA AGROALIMENTÀRIA,  
University of Girona  
irodriguezroda@icra.cat  
Expertise on Membrane Bioreactors Control and Modelling



Dear Editor,

Attached you will find the manuscript entitled “**Real-time optimization of the key filtration parameters in an AnMBR: urban wastewater mono-digestion vs. co-digestion with domestic food waste**” submitted for publication as an original article in *Waste Management*. All the authors mutually agree for submitting this manuscript to *Waste Management*, within the category 5.003: *Biological-anaerobic (anaerobic digestion)*. We confirm that it is an original work and that the information presented is not being considered for publication in any other journal.

This study describes a model-based method for real-time optimization of the key filtration parameters in a submerged anaerobic membrane bioreactor (AnMBR) treating urban wastewater (UWW) and a mixture of UWW and domestic food waste (FW). Hence, the main aim of this study was to design a competitive and feasible control system capable of enhancing filtration in industrial-scale AnMBR systems with minimum operating costs.

The novelty of this study lies in gaining more insight into the optimization of an AnMBR system at industrial scale. Indeed, to obtain representative results that could be extrapolated to full-scale plants, this study was carried out using data from an AnMBR system featuring industrial hollow-fibre (HF) membranes.

The important findings that must be highlighted are:

- The operating filtration cost after implementing the proposed control methodology was about €0.047 per influent m<sup>3</sup> when treating UWW (59.6 % corresponding to energy costs) and €0.067 per m<sup>3</sup> when adding FW due to higher fouling rates.
- FW also increased the biogas productivities, reducing the total costs to €0.035 per m<sup>3</sup>.
- Average downtimes for reversible fouling removal of 0.4 % and 1.6 % were obtained when treating UWW and a mixture of UWW and FW, respectively.
- The results confirm the capability of the proposed control system for optimizing the AnMBR performance when treating both UWW and a mixture of UWW and FW.

To the knowledge of the authors, no other study has been carried out for the optimization of the proposed process using the described methodology.

Yours sincerely,

Ángel Robles Martínez, PhD  
Departament d'Enginyeria Química, ETSE-UV.  
Universitat de València  
Avinguda de la Universitat s/n, 46100, Burjassot, València, Spain  
Tel.: +34 96 354 30 85  
E-mail: angel.robles@uv.es

## Highlights

- Average costs of €0.047 (UWW) and €0.067 per m<sup>3</sup> (UWW and FW) were obtained
- Energy costs accounted for 59.6% and 69.0% of the total costs respectively
- Average reversible fouling removal downtimes were 0.4% and 1.6% respectively
- Control strategy efficiently minimized filtration costs for both substrates

1           **Real-time optimization of the key filtration parameters in an AnMBR: urban**  
2           **wastewater mono-digestion vs. co-digestion with domestic food waste**

3           A. Robles <sup>a,\*</sup>, G. Capson-Tojo <sup>b</sup>, M. V. Ruano <sup>a</sup>, A. Seco <sup>a</sup>, J. Ferrer <sup>c</sup>

4  
5           <sup>a</sup> CALAGUA – Unidad Mixta UV-UPV, Departament d'Enginyeria Química, ETSE-UV,  
6           Universitat de València, Avinguda de la Universitat s/n, 46100, Burjassot, València, Spain.

7           <sup>b</sup> LBE, INRA, Univ. Montpellier, 102 avenue des Etangs, 11100, Narbonne, France

8           <sup>c</sup> CALAGUA – Unidad Mixta UV-UPV, Institut Universitari d'Investigació d'Enginyeria de  
9           l'Aigua i Medi Ambient – IIAMA, Universitat Politècnica de València, Camí de Vera s/n,  
10          46022, València, Spain

11          \* Corresponding author: tel. +34 96 354 30 85, e-mail: *angel.robles@uv.es*

12  
13          **Abstract**

14          This study describes a model-based method for real-time optimization of the key filtration  
15          parameters in a submerged anaerobic membrane bioreactor (AnMBR) treating urban  
16          wastewater (UWW) and UWW mixed with domestic food waste (FW). The method consists  
17          of three statistical analyses: (1) Morris screening method to identify the key filtration  
18          parameters; (2) Monte Carlo method to establish suitable initial control inputs values; and (3)  
19          optimization algorithm for minimizing the operating costs. The operating filtration cost after  
20          implementing the control methodology was €0.047 per m<sup>3</sup> (59.6% corresponding to energy  
21          costs) when treating UWW and €0.067 per m<sup>3</sup> when adding FW due to higher fouling rates.  
22          However, FW increased the biogas productivities, reducing the total costs to €0.035 per m<sup>3</sup>.  
23          Average downtimes for reversible fouling removal of 0.4% and 1.6% were obtained,  
24          respectively. The results confirm the capability of the proposed control system for optimizing

25 the AnMBR performance when treating both substrates.

26

## 27 **Keywords**

28 Anaerobic membrane bioreactor (AnMBR); process control; kitchen waste; fouling;  
29 modelling; urban wastewater

30

## 31 **1. Introduction**

32 Submerged anaerobic membrane bioreactors (AnMBRs) are amongst the most promising  
33 technologies for treatment of urban wastewater (UWW) (Ben and Semmens, 2002). When  
34 compared with traditional processes, such as conventional activated sludge system, AnMBRs  
35 offer several advantages (Judd and Judd, 2011; Raskin, 2012): (i) uncoupling of hydraulic  
36 retention time (HRT) and solids retention time (SRT), (ii) improvement of organic matter  
37 removal efficiency, (iii) reduction of the environmental footprint of the treatment process, (iv)  
38 production of a solids-free purified effluent, (v) smaller amounts of sludge produced due to  
39 the low biomass yield of anaerobic microorganisms, (vi) lower energy demands (no aeration  
40 needed), and (vii) energy recovery by biogas production. In addition, the co-digestion in  
41 AnMBRs of UWW with domestic food waste (FW) is a very interesting option which may  
42 serve to enhance the biogas productivities (*i.e.* by increasing the organic loading rate and the  
43 influent COD/SO<sub>4</sub><sup>2-</sup> ratio), thus improving the general economics of the treatment process  
44 (Becker et al., 2017). Moreover, this approach creates an opportunity for recycling energy and  
45 nutrients from both wastes (Kibler et al., 2018). This strategy also allows the valorization of  
46 domestic FW, whose anaerobic mono-digestion is known to be associated with several  
47 complications, such as accumulation of NH<sub>3</sub> and volatile fatty acids (VFAs) (Capson-Tojo et  
48 al., 2017, 2016).

49 However, a key issue exists that affects the economics of membrane filtration processes and

50 therefore its industrial applicability: membrane fouling (Deng et al., 2016; Sheets et al.,  
51 2015). Fouling reduces the permeability of the membrane, which leads to an increase in the  
52 operating and maintenance costs, jeopardizing the global performance (Judd and Judd, 2011).  
53 Moreover, previous studies have suggested that fouling issues tend to get worse if adding FW  
54 to the UWW (Pretel et al., 2016). Thus, if AnMBRs are to be a competitive alternative for  
55 UWW treatment from an economical point of view, minimizing the impact of membrane  
56 fouling is of critical importance. Therefore, one of the main challenges of this technology is to  
57 optimize the treatment performance (keeping high treatment flow rates) and the energy  
58 consumption (small physical cleaning intensities and periods) whilst minimizing the fouling  
59 effect. Particularly, avoiding irreversible fouling, which must be removed chemically and  
60 eventually determines the lifespan of the membranes, is of critical importance (Drews et al.,  
61 2009; Judd and Judd, 2011). Moreover, as the physical cleaning of the membranes can  
62 account for more than 75 % of the energetic consumption in AnMBRs (Verrecht et al., 2010),  
63 this step must also be optimized, reducing as much as possible its frequency.

64 In this respect, the development of advanced control systems is crucial for a successful  
65 optimization of the process performance in AnMBRs (Jimenez et al., 2015; Nguyen et al.,  
66 2015). Different studies have assessed theoretically (and sometimes validated experimentally)  
67 the energy and economical savings resulting from the implementation of different types of  
68 advanced control systems in aerobic membrane reactors (MBRs) (Drews et al., 2007;  
69 Huyskens et al., 2011). Mannina and Cosenza (2013) applied Monte Carlo simulations to  
70 compare the energy requirements, the effluent quality and the economic costs of five different  
71 scenarios based on an MBR model. Also, an ad-hoc platform constructed over the  
72 COST/Benchmark Simulation Model No. 1 (BSM1) (Coop, 2002) was applied to evaluate  
73 different control strategies in MBRs, using the energy requirements to assess the  
74 performances (Maere et al., 2011). Gabarron et al. (2014) compared different optimization



75 strategies applied to MBRs, reducing significantly the energy needs and the membrane  
76 fouling. Moreover, Ferrero et al. (2011a, 2011b, 2011c) reduced significant the energy  
77 requirements due to membrane scouring (up to 21%) by applying a knowledge-based control  
78 system based on a supervisory controller. Focusing on model-based control, Drews et al.  
79 (2009, 2007) created a control system based on a mathematical model that successfully  
80 improved the filtration efficiency. In addition, Busch et al. (2007) developed a run-to-run  
81 control system to optimize the filtration performance by adjusting the filtration variables after  
82 each filtration cycle. Recently, computational fluid dynamics simulations have also been  
83 applied to optimize membrane scouring and the hydrodynamics in airlift external circulation  
84 MBRs (Yang et al., 2017, 2016). These studies allowed a significant reduction of reversible  
85 fouling due to cake formation, thus maximizing the MBR performance.

86 However, so far few control strategies have been developed and validated to optimize the  
87 performance of AnMBRs for the treatment of UWW (Robles et al., 2013a). In Robles et al.  
88 (2013a), an upper layer fuzzy-logic controller efficiently kept low fouling rates, improving the  
89 process performance. In addition, a model-based optimization method has also been applied  
90 to improve the performance of AnMBRs treating UWW (Robles et al., 2014a). This method  
91 was effectively used for optimization of an advanced control system (consisting of an upper-  
92 layer fuzzy-logic controller), obtaining energy savings of up to 25 %. Nevertheless, to  
93 improve the economic viability of these systems, it is necessary to develop new control  
94 strategies that allow the filtration system to work under optimal conditions.

95 Among the different options that exist, the use of model-based control systems is of interest,  
96 not only to control the process performance, but also to predict it, allowing eventually its  
97 optimization from an energetic and/or economical approach (Batstone et al., 2015; Gernaey et  
98 al., 2004; Martin and Vanrolleghem, 2014). Nonetheless, the predictions based on models are  
99 never totally free of uncertainty because models are always a conceptual representation of

100 reality and are based on assumptions. Moreover, models need to be calibrated, a process that  
101 can be arduous. In this context, sensitivity analysis is a powerful tool that can be used for two  
102 main purposes: (i) quantifying the effects of the inputs on the outputs of the model and (ii)  
103 identifying the most relevant factors and those that can be disregarded, thus simplifying the  
104 calibration process (Pianosi et al., 2016).

105 Therefore, the objective of this study was to develop a model-based control strategy for real-  
106 time optimization of the performance of AnMBRs fed with UWW and a mixture of UWW  
107 and FW. Specifically, the strategy aimed at optimizing the operating mode of the filtration  
108 process in an AnMBR system by dynamic simulations using a previously validated filtration  
109 model. The real-time optimization strategy modified the key filtration parameters in the  
110 AnMBR according to the operating conditions of the plant, thus minimizing the operating  
111 costs in real-time. The applied model was based on an approach previously used for  
112 optimizing the input parameters of an advanced control system for filtration in AnMBRs  
113 (Robles et al., 2014a). The proposed optimization strategy consists of three sequential  
114 statistical methods: (i) a sensitivity analysis to find an identifiable input subset for the  
115 filtration process (Morris screening method) (Morris, 1991), (ii) a Monte Carlo procedure to  
116 find adequate initial conditions (using the trajectory-based random sampling technique) and  
117 (iii) an optimization algorithm to obtain the optimum input combination of values that  
118 minimizes the operating costs of the system.

119

## 120 **2. Materials and methods**

121 To accomplish the besought goal the first step of the process consisted in a sensitivity analysis  
122 that considers the different parameters susceptible to be optimized in a previously chosen  
123 model (Robles et al., 2013c, 2013d), thus selecting highly-influential parameters conforming  
124 the identifiable input subset to be optimized. Afterwards, the selection of adequate initial

125 conditions (those leading to local minimal operational costs) of the identifiable input subset  
126 was performed via the Monte Carlo method. Knowing these values, the optimization of the  
127 highly-influential operational parameters was carried out. With this purpose, an optimization  
128 algorithm was defined. This controller established, at every control time (CT), the set points for  
129 the operational parameters leading to the lowest costs of the filtration process. Finally, the  
130 reduction of the total costs of the filtration process after the implementation of the control  
131 system was assessed (with and without FW in the substrate).

### 132 *2.1. Description of the AnMBR plant*

133 The data used in this study to calibrate and validate the filtration model was obtained from an  
134 AnMBR that mainly consisted of an anaerobic reactor with a working volume of 0.9 m<sup>3</sup>  
135 connected to two membrane tanks. Each membrane tank had a working volume of 0.6 m<sup>3</sup> and  
136 included one ultrafiltration hollow-fibre membrane commercial system (PURON<sup>®</sup>, Koch  
137 Membrane Systems, 0.05 µm pore size, 31 m<sup>2</sup> total filtering area and outside-in filtration).  
138 The plant was fully automated and monitored online in real-time. In addition, the anaerobic  
139 sludge was sampled once a day to assess the filtration performance. The concentration of  
140 mixed liquor total solids (MLTS) was determined according to the Standard Methods (APHA,  
141 2005). A more precise description of the plant and its instrumentation (as well as the  
142 corresponding flow diagrams) can be found elsewhere (Robles et al., 2015, 2013b).

### 143 *2.1.2. Lower-layer controllers*

144 The lower-layer controllers implemented in the system that interact with the proposed  
145 optimization method are: (i) three PID controllers that adjust the rotating speed of the sludge  
146 recycling pump, the permeate pump and the biogas recycling blower used for membrane  
147 scouring by gas sparging; and (ii) one on–off controller that regulates the membrane operating  
148 stage by changing the position of the respective on–off valves and the flux direction of the  
149 permeate pump. A more precise description of the plant control system can be found

150 elsewhere (Robles et al., 2015).

## 151 2.2. Characteristics of the substrates

152 As aforementioned, the proposed model-based optimisation strategy was validated for an  
153 AnMBR treating UWW and a mixture of UWW and FW. To this aim, a filtration model was  
154 calibrated and validated using data from an AnMBR system that treated UWW and a mixture  
155 of UWW and FW. The UWW was the effluent from the pre-treatment step of the Carraixet  
156 WWTP (Valencia, Spain) and the FW was collected from canteens in the university (Moñino  
157 et al., 2016). The FW was grinded by an experimental set-up simulating a household grinding  
158 system. This set-up consisted on a grinded InSinkErator, model Evolution 100. Afterwards,  
159 the FW was pre-filtered using a mesh of 0.5 mm, similar to the one used for the UWW.  
160 Further details can be found elsewhere (Moñino et al., 2017).

## 161 2.3. Description of the filtration model

162 The filtration model used in this study is a semi-empirical model based on a classical  
163 resistance-in-series model (Robles et al., 2013c). This model is able to represent the dynamic  
164 evolution of the transmembrane pressure (TMP) by equations 1 and 2.

$$165 \quad TMP(t) = J_{net} \cdot \mu_p \cdot R_T \quad (\text{Eq. 1})$$

166 Where,  $TMP(t)$  is the TMP at time  $t$ ,  $\mu_p$  is the dynamic viscosity of the permeate and  $R_T$  is  
166 the total filtration resistance.

$$167 \quad R_T = R_M + R_C + R_I = R_M + \omega_C \cdot \alpha_C + \omega_I \cdot \alpha_I \quad (\text{Eq. 2})$$

168 Where,  $R_M$  is the resistance intrinsic to the membrane,  $R_C$  is the resistance of the cake that is  
168 formed on the surface of the membrane due to solid deposition,  $R_I$  is the added resistance due  
169 to irreversible membrane fouling,  $\omega_C$  is the mass of solids deposited on the membrane per  
170 membrane area,  $\alpha_C$  is the average specific resistance of the cake created,  $\omega_I$  is the mass of  
171 irreversible fouling normalized per membrane area and  $\alpha_I$  is the average specific resistance of

172 the irreversible fouling.

173 The dynamics of  $\omega_C$  and  $\omega_I$  were modelled using a black-box approach. With this purpose,  
174 three different components were defined:  $X_{TS}$  (MLTS),  $X_{mC}$  (cake dry mass in the membrane  
175 surface), and  $X_{mI}$  (irreversible fouling dry mass on the membrane surface). In addition, four  
176 kinetic physical processes were included in the model: (i) cake layer formation during  
177 filtration, (ii) cake layer removal by biogas sparging for membrane scouring, (iii) cake layer  
178 removal by back-flushing and (iv) irreversible fouling formation. A more precise description  
179 of the structure of the filtration model can be found elsewhere (Robles et al., 2014a).

180 The selected filtration model was calibrated and validated using experimental data from the  
181 above-introduced AnMBR plant when treating UWW and a mixture of UWW and FW.

#### 182 *2.4. Model-based optimization*

183 As aforementioned, the first stage of the optimization process is the selection of the  
184 operational parameters associated with the filtration process that are susceptible to be  
185 optimized dynamically. These variables are the biogas recycling flow-rate for membrane  
186 cleaning (BRF), the sludge recycling flow-rate into the membrane tanks (SRF), the duration  
187 of the filtration, relaxation and back-flushing stages ( $t_F$ ,  $t_R$  and  $t_{BF}$  respectively) and the  
188 initiation frequency and transmembrane flow of the back-flushing stage ( $f_{BF}$ ,  $J_{BF}$ ). It must be  
189 commented that the transmembrane flow during filtration ( $J_F$ ) has not been considered for the  
190 optimization. The reason is that this value will be fixed by the influent flow-rate to the  
191 system.

192 Considering these selected variables, the operating mode of the membranes can be  
193 represented by Figure 1A. As this figure shows, an alternation is established between the  
194 relaxation and the back-flushing stages. More precisely, if the number of filtration cycles ( $f$ ) is  
195 lower than  $f_{BF}$ , the system will alternate between filtration and relaxation cycles. However, if  
196  $f_{BF}$  is equal or overpasses  $f$ , the corresponding relaxation stage will be substituted by a back-

197 flushing stage. Figure 1B shows a schematic representation of the optimization methodology  
 198 applied in this study, which is based on a previously proposed real-time optimization  
 199 procedure and uses the previously introduced filtration model for calculations (Robles et al.,  
 200 2014a). First of all, the Morris screening method (Morris, 1991) was used to perform a global  
 201 sensitivity analysis (GSA) of the selected filtration model (step a) to identify the operational  
 202 parameters with high influence on the cost of the filtration process (step b). Once these  
 203 parameters were identified, the Monte Carlo procedure (see for instance Saltelli et al. (2000))  
 204 was applied to determine the optimal initial values of the evaluated parameters (step c). These  
 205 values are used to update the initial set-points of the operational parameters (step d), which  
 206 are transferred to the process (step e). After the transmission of the initial set-points, every CT  
 207 the optimization algorithm is started. In this work CT has been set to 1 hour. This supervisory  
 208 controller calculates the new optimal set-points for the highly-influential operational  
 209 parameters at each CT (step f) and transmits them (step g) to update again the set-points of the  
 210 process (steps d and e). To this aim, a cost objective function was used.

#### 211 *2.4.1. Description of the costs objective function*

212 To determine the costs related to energy consumption, the energy requirement of each process  
 213 was calculated and multiplied by the cost of energy ( $E_{COST}$ ; € per kWh). In this study  $E_{COST}$   
 214 was set to €0.138 per kWh, which corresponded to average electricity prices in Spain.

215 The energy requirements of the blower ( $W_{BRF}$ ) (adiabatic compression), sludge recycling  
 216 pump ( $W_{SRF}$ ) and permeate pump for filtration ( $W_{filtration}$ ) or back-flushing ( $W_{back-flusing}$ ) were  
 217 calculated as shown in Robles et al. (2014a).

218 The total energetic costs were lumped in a single variable ( $C_W$ ), which was calculated as the  
 219 sum of  $C_{BRF}$ ,  $C_{SRF}$  and  $C_{STAGE}$ , as shown in Equation 3:

$$C_W = C_{BRF} + C_{SRF} + C_{STAGE} = W_{BRF} \cdot E_{COST} + W_{SRF} \cdot E_{COST} + W_{STAGE} \cdot E_{COST} \quad (\text{Eq. 3})$$

220 Where,  $C_W$  is the total energetic cost,  $C_{BRF}$  is the operating cost of membrane scouring by  
221 biogas sparging,  $C_{SRF}$  is the operating cost of pumping the sludge,  $C_{STAGE}$  is the operating cost  
222 of pumping permeate during the respective operating stage (*i.e.* filtration or back-flushing),  
223 Finally, in order to determine the combination of operational set-points that lead to the  
224 minimal value of the total operating costs ( $C_{TOTAL}$ ; € per  $m^3$ ), Equation 4 was applied.

$$C_{TOTAL} = C_W + C_{REAGENTS} + C_{LIFESPAN} \quad (\text{Eq. 4})$$

225 Where,  $C_W$  is the total energetic cost,  $C_{REAGENTS}$  is the proportional cost of reagents needed to  
226 clean the irreversible fouling produced during filtration and  $C_{LIFESPAN}$  is the cost of membrane  
227 replacement due to irreversible fouling.  $C_{REAGENTS}$  and  $C_{LIFESPAN}$  were calculated as shown in  
228 Robles et al. (2014a).

#### 229 2.4.2. Global sensitivity analysis: Morris screening method

230 In this study the Morris screening method (Morris, 1991) has been applied to perform the  
231 GSA. This method is a one-factor-at-a-time process based on the generation of representative  
232 matrices of the combinations of values of the parameters to evaluate through a random  
233 sampling. From the matrices it determines the distribution of elemental effects ( $EE_i$ ) of each  
234 input factor on the model output. Finally, the  $EE_i$  distribution ( $F_i$ ) for each input factor is  
235 analyzed to determine the relative importance of the input factors and obtain a good  
236 approximation of a GSA.

237 The selected statistical parameters to evaluate these distributions were: the standard deviation  
238 ( $\sigma$ ) and the absolute mean ( $\mu^*$ ) (see for instance Saltelli et al. (2000) and Campolongo et al.  
239 (2007)).

240 In order to elucidate which operational parameters are the most influential on the total  
241 filtration cost, the output variable for the GSA in this study was  $C_{TOTAL}$  (Eq. 4).

242 A more precise description of the GSA applied in this study can be found elsewhere (Robles

243 et al., 2014b).

#### 244 *2.4.3. Initial values of the operation parameters: Monte Carlo method*

245 The Monte Carlo method was used for the selection of initial values of the operational  
246 parameters close to the minimum (locally) of the function to minimize. This has two main  
247 benefits: (i) it improves the results of the dynamical optimization given by the controller and  
248 (ii) it gives optimal values of the non-influential parameters, further improving the  
249 minimization of  $C_{TOTAL}$ . Therefore, the Monte Carlo method was applied as a previous step  
250 before the dynamic optimization. The Monte Carlo method consisting on trajectory-based  
251 random sampling was used in this study. Hence, the combination of the operational  
252 parameters giving the minimum operating cost (Eq. 4) was selected as the initial values of the  
253 model-based supervisory controller.

#### 254 *2.4.4. Simulation strategy and model calibration*

255 MATLAB<sup>®</sup> was used to simulate the filtration process using the previously-introduced model.  
256 The Runge-Kutta method (ode45 function in MATLAB<sup>®</sup>) was used as integration method for  
257 solving the differential equations in the model. The model was calibrated using experimental  
258 results from operation with both substrates.

#### 259 *2.4.5. Simulations for real-time dynamic optimization of the filtration process*

260 The dynamic optimization of the filtration process was carried out using the costs equation  
261 (Eq. 4) as objective function. The optimization algorithm was applied by using the trust  
262 region approach (Coleman and Li, 1996), based on the Newton method (LSQNONLIN  
263 function in MATLAB<sup>®</sup>) and the Runge-Kutta method (ode45 function in MATLAB<sup>®</sup>).

#### 264 *2.4.6. Implementation of the Morris and Monte Carlo methods*

265 In order to obtain results that could be extrapolated to different situations, MLTS  
266 concentrations in the entrance of the membrane tanks was ranged from 10 to 20 g·l<sup>-1</sup> during  
267 simulation. In addition, to take into account the typical fluctuations of the flow rate entering a



268 WWTP, the net transmembrane flow ( $J_{\text{net}}$ ) was also varied. For each concentrations of MLTS,  
269  $J_{\text{net}}$  was modified from 4 to 12 LMH ( $\text{l}\cdot\text{h}^{-1}\cdot\text{m}^{-2}$ ), following the influent pattern from the model  
270 BSM1 (Jeppsson et al., 2006).

271 The average values of the operational parameters evaluated in this study are shown in Table 1.  
272 In addition, the uncertainty considered for the sensitivity analysis (minimum and maximum  
273 values) is also presented. The range of values for the set-points of these parameters was  
274 established according to a uniform distribution. Finally, the results of the Monte Carlo  
275 procedure (which will be discussed afterwards) are also shown in Table 1.

#### 276 *2.4.7. Optimization algorithm*

277 Using UWW as substrate, the performance of the controller (based on the optimization  
278 algorithm) was evaluated by simulation using the filtration model described above. The  
279 simulation accounted for 24 h of continuous operation and was carried out at four different  
280 MLTS concentrations entering the membrane tanks: 11, 13, 15 and  $17\text{ g}\cdot\text{l}^{-1}$ . For the co-  
281 digestion experiment (mixture of UWW and FW), the performance of the supervisory  
282 controller was also evaluated in an operational period of 24 h with a MLTS concentration of  
283  $17\text{ g}\cdot\text{l}^{-1}$ . This allowed the comparison between both feeding strategies (*i.e.* UWW and mixture  
284 of UWW and FW).

285 During the simulations  $J_{\text{net}}$  varied according to the dynamic of BSM1 influent (Jeppsson et al.,  
286 2006) (see e-supplementary data).

287 As aforementioned, the CT was set to 1 hour. The computational cost for optimizing  
288 dynamically the process was between 1 to 3 minutes (using a PC Intel<sup>®</sup> CORE<sup>™</sup> i5 with 8  
289 GHz of RAM).

### 290 **3. Results and discussion**

#### 291 *3.1. Calibration of the model*

292 Before the application of the model, it was previously calibrated and validated using data

293 obtained in the AnMBR plant under a wide range of operational conditions. More precisely,  
294 the model was validated for different concentrations of MLTS entering the membrane tanks  
295 ( $10\text{-}30\text{ g}\cdot\text{l}^{-1}$ ), different  $J_{\text{net}}$  ( $4\text{-}6\text{ LMH}$ ) and different specific demands of gas per square meter  
296 of membrane ( $\text{SDG}_m$ ) ( $0.1\text{-}0.5\text{ m}^3\cdot\text{h}^{-1}\cdot\text{m}^{-2}$ , equivalent to BRFs of  $3\text{-}15\text{ m}^3\cdot\text{h}^{-1}$ ). The model was  
297 able to predict precisely the behavior of the membrane during the studied operational  
298 conditions ( $R$  of  $0.989$ ). A more precise description of the calibration and validation of the  
299 model applied can be found elsewhere (Moñino et al., 2017).

### 300 *3.2. Sensitivity analysis*

#### 301 *3.2.1. Treating urban wastewater*

302 The rankings for the operational parameters according to the sensitivity measurements  
303 obtained ( $\mu^*$  and  $\sigma$ ) are presented in Table 2. Only the results for the optimized number of  
304 evaluated trajectories ( $r_{\text{opt}}$ ) are shown.

305 Hierarchical clustering analysis (HCA; R software version 3.2.5.) of the  $\mu^*$  presented in Table  
306 2 and the ones obtained during  $r_{\text{opt}}$  determination resulted in three differentiated clusters  
307 formed according to the influence of the studied parameters on the model output (see e-  
308 supplementary data): (i) BRF, with a much higher value of  $\mu^*$  when compared with the other  
309 parameters, indicating its great importance for the process costs; (ii)  $f_{\text{BF}}$ ,  $t_{\text{BF}}$ ,  $t_{\text{F}}$  and SRF, with  
310 values of  $\mu^*$  that indicate a significant relative influence on the process costs; and (iii)  $t_{\text{R}}$  and  
311  $J_{\text{BF}}$ , with a low relative importance. According to these results, 5 parameters were identified  
312 as highly influential on the process costs: (i) BRF ( $\mu^* = 1.253$  and  $\sigma = 1.856$ ); (ii)  $f_{\text{BF}}$  ( $\mu^* =$   
313  $0.770$  and  $\sigma = 2.220$ ); (iii)  $t_{\text{F}}$  ( $\mu^* = 0.724$  and  $\sigma = 1.921$ ); (iv)  $t_{\text{BF}}$  ( $\mu^* = 0.574$  and  $\sigma = 1.210$ );  
314 and (v) SRF ( $\mu^* = 0.464$  and  $\sigma = 1.584$ ). To allow a visual identification of these parameters, a  
315 graphical representation of the results of the sensitivity parameters ( $\mu^*$  and  $\sigma$ ) at  $r_{\text{opt}}$  can be  
316 found in the Electronic Annex. Both the clustering and the graphical results suggest a high  
317 influence of BRF, SRF,  $t_{\text{F}}$ ,  $t_{\text{BF}}$  and  $f_{\text{BF}}$  on the cost of the process. Therefore, in this study they

318 have been optimized dynamically as a function of the operational conditions. On the other  
319 hand, as  $t_R$  and  $J_{BF}$  present low values of  $\mu^*$  and  $\sigma$ , it can be considered that their influence on  
320 the total costs is low. Thus, their set-points were considered to be constant, keeping the initial  
321 values given by the Monte Carlo method. In addition, the GSA results allow evaluating the  
322 mathematical relationship between each parameter and the total costs. Due to their relative  
323 high values of both  $\mu^*$  and  $\sigma$ , the effects of BRF, SRF,  $t_F$ ,  $t_{BF}$  and  $f_{BF}$  can be classified as non-  
324 linear.

325 The huge influence of BRF was related to the high energy consumption of this process. Thus,  
326 while an adequate value of BRF allows minimizing the solid cake formation, the irreversible  
327 fouling rates and the costs associated with biogas recirculation, too high values increase  
328 greatly the total costs of the filtration process. Concerning SRF, this parameter affects, not  
329 only the costs associated with sludge pumping, but also  $MLTS_{MT}$  at a given  $J_{net}$ . It is  
330 important to consider that changes of the  $MLTS_{MT}$  modify also the BRF requirements. In  
331 addition,  $t_F$  affects the amount of solids that are deposited onto the surface of the membranes.  
332  $t_F$  also influences the net water treatment flow, thus determining the normalized profitability  
333 of the process (expressed in € per  $m^3$ ). Finally,  $t_{BF}$  and  $f_{BF}$  modify the extent of permeability  
334 recovery of the membranes. This is related to a partial or total removal of the solid cake.  
335 However, it must also be considered that high values of  $t_{BF}$  and  $f_{BF}$  decrease  $J_{net}$  and increase  
336 the non-filtration period of the AnMBR.

### 337 *3.2.2. Treating urban wastewater and food waste*

338 The values of the sensitivity measurements ( $\mu^*$  and  $\sigma$ ) obtained for the optimized number of  
339 evaluated trajectories ( $r_{opt} = 40$ ) when using UWW and FW as substrates are presented in  
340 Table 2. The corresponding HCA (see e-supplementary data) resulted in very similar clusters  
341 when compared to the process treating only UWW. In this case, 5 main clusters were  
342 obtained: (i) BRF, again with a much higher value of  $\mu^*$  when compared with the other

343 parameters; (ii)  $f_{BF}$ , with higher relative values when compared to treatment of only UWW;  
344 (iii)  $t_{BF}$  and  $t_F$ , also with values of  $\mu^*$  that indicate a significant relative influence; (iv) SRF  
345 and  $t_R$ , with a low relative influence; and (v)  $J_{BF}$ , with a very low relative importance. The  
346 similar responses of the systems fed with UWW and the mixture of UWW and FW confirm  
347 the applicability of the optimization methodology evaluated in this study to both substrates. In  
348 order to allow an un-biased comparison of the performances of the supervisory controller  
349 using both substrates, the same five operational parameters were identified as influential:  
350 BRF,  $f_{BF}$ ,  $t_{BF}$ ,  $t_F$  and SRF. However, it must be considered that the clustering results suggest  
351 that in this case SRF could also be kept constant, reducing even more the computational costs.  
352 As for the case using UWW as substrate, a graphical representation of the obtained sensitivity  
353 rankings treating the UWW and FW mixture is presented in the Electronic Annex.

### 354 *3.3. Initial parameter estimation via the Monte Carlo method*

355 As aforementioned, the Monte Carlo method was used to estimate the initial values of the  
356 different operational parameters object of study when applying both feeding strategies (*i.e.*  
357 UWW and mixture of UWW and FW). The total filtration cost varied greatly, with values  
358 ranging between €0.04 per  $m^3$  and €0.40 per  $m^3$ . Therefore, it can be concluded that the total  
359 costs can be effectively minimized by selecting the proper set-points of the selected  
360 operational parameters.

361 The obtained results, which correspond to the combination leading to minimum local costs,  
362 are presented in Table 1 (column Monte Carlo Results). However, it is important to highlight  
363 that the Monte Carlo method cannot give an optimal combination of the operational  
364 parameters. This occurs because of the discrete variation of the values of the evaluated  
365 parameters chosen to carry out the simulations. Nevertheless, as the used sampling procedure  
366 aims at covering all the domain of variation of the parameters, the cost is locally minimized.  
367 Starting from the initial combination given by the Monte Carlo method, the selected

368 parameters were optimized dynamically throughout the operational period.

### 369 3.4. Performance of the supervisory controller

#### 370 3.4.1. Treating urban wastewater

371 Figure 2 shows the values of BRF, SRF,  $t_F$  and  $t_{BF}$  optimized by the controller during the  
372 simulations performed with a MLTS concentration entering the membrane tank of  $17 \text{ g}\cdot\text{l}^{-1}$  and  
373 the transmembrane fluxes shown in the e-supplementary data. This condition is presented  
374 because of two main reasons: (i) it allows comparing the performance of the controller using  
375 both substrates and (ii) it is the worst case scenario, meaning that in reality the performance  
376 should be improved, with less fouling and lower filtration costs when reducing  $\text{MLTS}_{\text{MT}}$ .

377 As shown in Figure 2A, the value of BRF followed a very similar pattern when compared to  
378  $J_{\text{net}}$ . This occurred because the controller established higher values of BRF in the periods  
379 when the treatment flow rate was the highest (10-13 hours). During those flow peaks, the  
380 velocity of solid deposition on the surface of the membrane was much higher than at regular  
381 operation and therefore the controller had to increase considerably BRF to keep the TMP at  
382 appropriate values. In addition, Figure 2A also shows that the value of BRF was reduced  
383 when the treatment flow decreased, reaching even the minimum BRF value allowed in the  
384 AnMBR plant ( $4 \text{ m}^3\cdot\text{h}^{-1}$ ). These conditions corresponded to the minimal membrane fouling  
385 propensity, but were also associated with low agitation of the sludge in the membrane tanks,  
386 leading to a reduction in the efficiency of the process of physical cleaning by biogas sparging.  
387 A correlation matrix including the optimized parameters,  $\text{MLTS}_{\text{MT}}$ ,  $J_{\text{net}}$ , TMP, the energy  
388 requirements and the filtration costs with UWW as substrate (see e-supplementary data; R  
389 software version 3.2.5.) verified the positive correlation observed between  $J_{\text{net}}$ , TMP and  
390 BRF.

391 Regarding SRF, Figure 2A shows a similar behavior to that observed for BRF. The controller  
392 increased SRF at higher  $J_{\text{net}}$  to keep  $\text{MLTS}_{\text{MT}}$  at adequate levels. Again, the correlation matrix

393 verified the correlation existing between BRF and SRF.

394 Concerning  $t_F$  and  $t_{BF}$ , it can be observed in Figure 2B that in this case these variables did not  
395 follow a pattern similar to that of  $J_{net}$ . However, a variation of these parameters occurred  
396 through the operational period studied. Interestingly, the periods when  $t_F$  and  $t_{BF}$  varied the  
397 most were those when BRF and SRF showed their lowest values (*i.e.* 5-9 h and 19-24 h). This  
398 indicates that, when the controller could not further optimize BRF and SRF, it modified the  
399 parameters with lower influence (*i.e.*  $t_F$  and  $t_{BF}$ ) to further minimize the total filtration costs.

400 No linear correlations were observed between  $t_F$  and  $t_{BF}$  and any other studied  
401 parameter/variable (see e-supplementary data). The last parameter to be discussed ( $f_{BF}$ )  
402 remained relatively constant, around 1 BF every 10 F cycles (see Figure 3).

403 Figure 3 represents the evolution of the TMP and the sequence of operational stages (F, R and  
404 BF) performed during the simulation at  $17 \text{ g}\cdot\text{l}^{-1}$  MLTS entering the membrane tanks.

405 As it can be observed, the operational mode varied according to the duration of the stages ( $t_F$   
406 and  $t_{BF}$ ). In addition, by increasing SRF and BRF (Figure 2A) during the periods most prone  
407 to fouling (hours 10-12), the supervisory controller was able to keep the TMP under the  
408 maximum limits established by the provider (*i.e.* 0.6 bars).

409 *3.4.2. Treating urban wastewater and food waste*

410 Figure 4 shows the values of BRF, SRF,  $t_F$  and  $t_{BF}$  optimized by the supervisory controller  
411 when treated UWW and FW. As for the operation with UWW as substrate (Figure 2A), the  
412 values of BRF and SRF varied according to the variations in  $J_{net}$  (see e-supplementary data).

413 As previously, the controller established higher values of both parameters at the points of  
414 highest  $J_{net}$  (10-13 hours). This period corresponded to the greatest rates of solids deposition  
415 onto the membranes. Therefore, the controller increased BRF to reduce the fouling rate and  
416 increased also SRF to minimize  $MLTS_{MT}$ .

417 In addition, it can be observed in Figure 4B that the values of  $t_F$  are lower than those obtained

418 with UWW as substrate (Figure 2B). Interestingly, the opposite occurred for  $t_{BF}$ , whose length  
419 was higher with the mixture of UWW and FW. This was related to a more intense fouling  
420 caused by the FW, which led to longer BF periods to remove the cake layer from the  
421 membrane surface. Moreover,  $f_{BF}$  increased from 1 BF every 10 F cycles to 1 BF every 4 F  
422 cycles (data not shown). Longer  $t_{BF}$  and higher  $f_{BF}$  with FW led to an increase of the  
423 downtime for reversible fouling removal. The average downtime for reversible fouling  
424 removal increased from 0.4 % (UWW) to 1.6 % (UWW and FW) of the total operational  
425 period. Nevertheless, it must be considered that these are low values which were achieved as a  
426 result of the controller action. As example, previous studies have reported minimum values of  
427 2.4 % of downtime when treating UWW in an automatically-tuned advanced control system  
428 for AnMBRs (Robles et al., 2014a).

429 It must be mentioned that the corresponding correlation matrix (see e-supplementary data)  
430 was very similar to that obtained for UWW as substrate, verifying that the controller  
431 responded in a similar manner for both substrates. Also, as the evolution of the TMP and the  
432 different stages simulated using the substrate mixture were similar to that of UWW treatment  
433 (Figure 3), these values are not presented.

### 434 3.5. Total energy consumption

435 Figure 5A shows the evolution of the energy requirements of the filtration process after the  
436 implementation of the supervisory controller at  $17 \text{ g}\cdot\text{l}^{-1}$  MLTS entering the membrane tank  
437 with UWW as substrate. As it can be observed, the main contributor to the energy  
438 consumption of the system was  $W_{BRF}$ , accounting in average for 80 % of the total energy  
439 requirements and up to 87 % at the highest  $J_{net}$ . In addition,  $W_{BRF}$  (thus  $W_{TOTAL}$ ) shows a  
440 similar pattern to that observed for  $J_{net}$ . In fact, both variables were strongly correlated (see e-  
441 supplementary data). While during the periods of low inflow to the plant (*i.e.* hours 2-9)  
442  $W_{TOTAL}$  reached  $0.13 \text{ kWh}\cdot\text{m}^{-3}$  (with  $W_{BRF}$  accounting for 67 %), this value increased up to

443  $0.34 \text{ kWh}\cdot\text{m}^{-3}$  (with  $W_{\text{BRF}}$  accounting for 87 %) at high  $J_{\text{net}}$  (*i.e.* hours 9-12). At this point it  
444 must be mentioned that the results shown in this study were obtained with a model calibrated  
445 using considerably dirty membranes (*i.e.* the membranes were already strongly irreversibly  
446 fouled). Therefore, the energy requirements presented correspond to a very unfavorable  
447 scenario and it can be expected that their values will be considerably lower when operating  
448 with clean membranes. Nevertheless, the proposed control strategy allowed keeping the  $W_{\text{BRF}}$   
449 within low values (around  $0.18 \text{ kWh}\cdot\text{m}^{-3}$ ). More precisely, the supervisory control system led  
450 to savings of around 50 % of the energy required for membrane scouring when compared to  
451 non-optimized cyclic operation of the same AnMBR plant ( $0.36 \text{ kWh}\cdot\text{m}^{-3}$ ) (Robles et al.,  
452 2013a). By coupling model-based control systems with fuzzy-logic advanced supervisory  
453 control, consumptions of  $0.15 \text{ kWh}\cdot\text{m}^{-3}$  (Robles et al., 2013a) and  $0.12 \text{ kWh}\cdot\text{m}^{-3}$  (Robles et  
454 al., 2014a) were achieved. The value obtained in this study was slightly higher ( $0.18 \text{ kWh}\cdot\text{m}^{-3}$ ).  
455 However, it must be considered that in this case only a model must be calibrated, which  
456 can be continuously optimized by retrofitting. In addition, if the model is properly calibrated  
457 this control strategy is more straight-forward and the control action is faster when compared  
458 to the previous control strategies, which require more computational capacity.

459 When paying attention to the average energy requirements of the AnMBR after the  
460 implementation of the control system (Table 3), it can be observed that from the total  
461 consumption of  $0.20 \text{ kWh}\cdot\text{m}^{-3}$  (operating at  $17 \text{ g}\cdot\text{l}^{-1}$  MLTS entering the membrane tanks), 79.7  
462 % corresponded to  $W_{\text{BRF}}$ , 16.9  $\text{kWh}\cdot\text{m}^{-3}$  to  $W_{\text{SRF}}$ , 9.53 % to  $W_{\text{back-flushing}}$  and 4.77 % to  
463  $W_{\text{filtration}}$ .

464 The results presented in Figure 5 and Table 3 show that the energy required to clean  
465 physically the membranes by biogas sparging ( $W_{\text{BRF}}$ ) represents the main consumption of  
466 energy in AnMBRs. Thus, there is a clear need to optimize this particular process.

467 Figure 5B and Table 3 also show the energy consumption of the filtration process treating



468 UWW and FW. In this case, the average total requirement was  $0.34 \text{ kWh}\cdot\text{m}^{-3}$ , with a  
469 maximum value of  $0.58 \text{ kWh}\cdot\text{m}^{-3}$ . The average proportion of  $W_{\text{BRF}}$  accounted for 88.5 %,   
470 indicating the need of optimizing BRF for each specific process.

471 The higher average  $W_{\text{TOTAL}}$  when adding FW ( $0.34$  vs.  $0.20 \text{ kWh}\cdot\text{m}^{-3}$ ) was related to the  
472 aforementioned increase of the fouling rate in the membranes, which implied longer non-  
473 filtration periods, thus reducing the net volume of water treated per unit of membrane surface.

474 However, it must be considered that the addition of FW also led to a higher energy recovery  
475 due to an increase of the biogas production. With a SRT of 70 days at a temperature of  $27 \text{ }^\circ\text{C}$ ,  
476 the volumetric methane production was up to  $72 \text{ l}_{\text{CH}_4}\cdot\text{m}^{-3}$  using UWW as substrate (Pretel et  
477 al., 2016). When adding FW, this value increased up to  $147 \text{ l}_{\text{CH}_4}\cdot\text{m}^{-3}$  which, assuming a  
478 percentage of methane recovery of 80 %, was translated into an increase of the energy  
479 recovery of  $0.20 \text{ kWh}\cdot\text{m}^{-3}$ . Taking this value into account, the energy requirements of the  
480 filtration process are lowered from  $0.34 \text{ kWh}\cdot\text{m}^{-3}$  to  $0.14 \text{ kWh}\cdot\text{m}^{-3}$ , even when operating with  
481 strongly fouled membranes. Thus, the addition of FW led to a global energy savings of 30 %  
482 when compared to the treatment of UWW as sole substrate. Therefore, it can be concluded  
483 that, even if FW was added into the UWW, the supervisory control system allowed operating  
484 the AnMBR at low energy costs.

### 485 *3.6. Total costs*

486 Figure 6A shows the evolution of the operational and maintenance costs of the filtration  
487 system after the implementation of the supervisory controller treating UWW at  $17 \text{ g}\cdot\text{l}^{-1}$   
488 MLTS. As it can be observed,  $C_{\text{W}}$  represented the main cost of the process, accounting for an  
489 average of 60 % of the total cost. This clearly emphasizes the need to optimize the operational  
490 conditions to minimize the energy demand of the system. However, in the period of peak  $J_{\text{net}}$   
491 (hours 9-10) the ensemble of  $C_{\text{REAGENTS}}$  and  $C_{\text{LIFESPAN}}$  represented up to 90 % of the total  
492 costs. This was related to a more intense irreversible fouling occurring in this period of high-

493 rate filtration, which caused an increase in the amounts of chemicals required to clean the  
494 membranes and lowered the membrane lifespan, raising the associated costs.  
495 Regarding the average costs, the results operating at  $17 \text{ g}\cdot\text{l}^{-1}$  MLTS entering the membranes  
496 are presented in Table 4. After the implementation of the control system,  $C_{\text{TOTAL}}$  was €0.047  
497 per  $\text{m}^3$ , with  $C_{\text{W}}$ ,  $C_{\text{REAGENTS}}$  and  $C_{\text{LIFESPAN}}$  representing the 59.6, 17.0 and 23.4 %,  
498 respectively.  
499 These values corroborate that  $C_{\text{W}}$  represents the main filtration costs during regular operation.  
500 In addition, as it has been already mentioned, the membranes used in this study were strongly  
501 fouled, and therefore lower costs are expected in real operation. Thus, the values of these  
502 latter costs should be lower in full-scale plants, further reinforcing the great importance of  
503 optimizing the energy requirement in AnMBR plant.  
504 Figure 6B and Table 4 present the costs corresponding to the co-digestion system (UWW and  
505 FW). As shown, the obtained pattern was very similar to that obtained for treatment of UWW.  
506 However, in this case the average filtration cost corresponded to €0.067 per  $\text{m}^3$ , with  $C_{\text{W}}$   
507 accounting for 69 % of this value. The higher value of  $C_{\text{TOTAL}}$  when adding FW is again  
508 related to a higher fouling rate in the co-digestion system, which led to higher costs associated  
509 with the mechanical cleaning of the membrane. This is further suggested by the higher  $C_{\text{W}}$   
510 values (€0.046 per  $\text{m}^3$  with FW vs. €0.028 per  $\text{m}^3$  with only UWW).  
511 However, when taking into account the economical profit related to the higher volumetric  
512 methane production when adding FW to the UWW,  $C_{\text{TOTAL}}$  is reduced to €0.035 per  $\text{m}^3$ ,  
513 meaning that FW addition led a relative economic saving of 26 % of the filtration costs (when  
514 compared with the AnMBR system treating only UWW).

515

#### 516 **4. Conclusions**

517 The proposed methodology enabled identifying the most influential filtration parameters and

518 selecting proper initial set points for their optimization. The controller allowed a real-time  
519 optimization of these set-points, obtaining an energy demand of  $0.20 \text{ kWh}\cdot\text{m}^{-3}$  (79.7%  $W_{\text{BRF}}$ )  
520 and a cost of  $\text{€}0.047 \text{ per m}^3$  (59.6%  $C_{\text{W}}$ ) when treating UWW. The addition of FW increased  
521 the energy demand and the costs ( $0.34 \text{ kWh}\cdot\text{m}^{-3}$  and  $\text{€}0.067 \text{ per m}^3$ ) due to higher fouling  
522 intensity, but also led to the production of more biogas. The obtained results confirm the  
523 applicability of the proposed control system for optimizing the AnMBR performance when  
524 treating both substrates.

525

## 526 **Acknowledgements**

527 This research work was possible thanks to financial support from Generalitat Valenciana  
528 (project PROMETEO/2012/029) which is gratefully acknowledged. Besides, support from  
529 FCC Aqualia participation in INNPRONTA 2011 IISIS IPT-20111023 project (partially  
530 funded by The Centre for Industrial Technological Development (CDTI) and from the  
531 Spanish Ministry of Economy and Competitiveness) is gratefully acknowledged.

532

## 533 **References**

- 534 APHA, 2005. Standard Methods for the Examination of Water and Wastewater. American  
535 Public Health Association, Washington, DC.
- 536 Batstone, D.J., Puyol, D., Flores-Alsina, X., Rodríguez, J., 2015. Mathematical modelling of  
537 anaerobic digestion processes: applications and future needs. *Rev. Environ. Sci.*  
538 *Bio/Technology* 14, 595–613.
- 539 Becker, A.M., Yu, K., Stadler, L.B., Smith, A.L., 2017. Co-management of domestic  
540 wastewater and food waste: A life cycle comparison of alternative food waste diversion  
541 strategies. *Bioresour. Technol.* 223, 131–140.
- 542 Ben, A., Semmens, M., 2002. Membrane bioreactors for wastewater treatment and reuse: a  
543 success story. *Water Sci. Technol.* 47, 1–5.
- 544 Busch, J., Cruse, A., Marquardt, W., 2007. Run-to-run control of membrane filtration  
545 processes. *AIChE J.* 53, 2316–2328.
- 546 Campolongo, F., Cariboni, J., Saltelli, A., 2007. An effective screening design for sensitivity  
547 analysis of large models. *Environ. Model. Softw.* 22, 1509–1518.

- 548 Capson-Tojo, G., Rouez, M., Crest, M., Steyer, J.-P., Delgenès, J.-P., Escudié, R., 2016. Food  
549 waste valorization via anaerobic processes: a review. *Rev. Environ. Sci. Bio/Technology*  
550 15, 499–547.
- 551 Capson-Tojo, G., Rouez, M., Crest, M., Trably, E., Steyer, J., Bernet, N., Delgenes, J.,  
552 Escudié, R., 2017. Kinetic study of dry anaerobic co-digestion of food waste and  
553 cardboard for methane production. *Waste Manag.* 69, 470–479.
- 554 Coleman, T.F., Li, Y., 1996. An interior trust region approach for nonlinear minimization  
555 subject to bounds. *SIAM J. Optim.* 6, 418–445.
- 556 Coop, J.B., 2002. *The COST Simulation Benchmark: Description and Simulator Manual.*  
557 Luxembourg.
- 558 Deng, L., Guo, W., Ngo, H.H., Zhang, H., Wang, J., Li, J., Xia, S., Wu, Y., 2016. Biofouling  
559 and control approaches in membrane bioreactors. *Bioresour. Technol.* 221, 656–665.
- 560 Drews, A., Arellano-Garcia, H., Schöneberger, J., Schaller, J., Kraume, M., Wozny, G., 2007.  
561 Improving the efficiency of membrane bioreactors by a novel model-based control of  
562 membrane filtration, in: *17th European Symposium on Computer Aided Process*  
563 *Engineering – ESCAPE.* pp. 345–350.
- 564 Drews, A., Arellano-Garcia, H., Schöneberger, J., Schaller, J., Wozny, G., Kraume, M., 2009.  
565 Model-based recognition of fouling mechanisms in membrane bioreactors. *Desalination*  
566 236, 224–233.
- 567 Ferrero, G., Monclus, H., Buttiglieri, G., Comas, J., Rodriguez-Roda, I., 2011. Automatic  
568 control system for energy optimization in membrane bioreactors. *Desalination* 268, 276–  
569 280.
- 570 Ferrero, G., Monclus, H., Buttiglieri, G., Gabarron, S., Comas, J., Rodriguez-Roda, I., 2011.  
571 Development of an algorithm for air-scour optimization in Membrane Bioreactors, *IFAC*  
572 *Proceedings Volumes (IFAC-PapersOnline).* IFAC.
- 573 Ferrero, G., Monclús, H., Sancho, L., Garrido, J.M., Comas, J., Rodríguez-Roda, I., 2011. A  
574 knowledge-based control system for air-scour optimisation in membrane bioreactors.  
575 *Water Sci. Technol.* 63, 2025–2031.
- 576 Gabarron, S., Ferrero, G., Dalmau, M., Comas, J., Rodriguez-Roda, I., 2014. Assessment of  
577 energy-saving strategies and operational costs in full-scale membrane bioreactors. *J.*  
578 *Environ. Manage.* 134, 8–14.
- 579 Gernaey, K. V., van Loosdrecht, M.C., Henze, M., Lind, M., Jørgensen, S.B., 2004. Activated  
580 sludge wastewater treatment plant modelling and simulation: state of the art. *Environ.*  
581 *Model. Softw.* 19, 763–783.
- 582 Huyskens, C., Brauns, E., Van Hoof, E., Diels, L., De Wever, H., 2011. Validation of a  
583 supervisory control system for energy savings in membrane bioreactors. *Water Res.* 45,  
584 1443–1453.
- 585 Jeppsson, U., Rosen, C., Alex, J., Copp, J., Gernaey, K. V., Pons, M.N., Vanrolleghem, P. a.,  
586 2006. Towards a benchmark simulation model for plant-wide control strategy  
587 performance evaluation of WWTPs. *Water Sci. Technol.* 53, 287–295.
- 588 Jimenez, J., Latrille, E., Harmand, J., Robles, A., Ferrer, J., Gaida, D., Wolf, C., Mairet, F.,  
589 Bernard, O., Alcaraz-Gonzalez, V., 2015. Instrumentation and control of anaerobic  
590 digestion processes: a review and some research challenges. *Rev. Environ. Sci.*

591 Bio/Technology 14, 615–648.

592 Judd, S., Judd, C., 2011. The MBR Book: Principles and applications of membrane  
593 bioreactors for water and wastewater treatment, 2nd ed. Elsevier, London (UK).

594 Kibler, K.M., Reinhart, D., Hawkins, C., Motlagh, A.M., Wright, J., 2018. Food waste and the  
595 food-energy-water nexus: A review of food waste management alternatives. Waste  
596 Manag., In Press.

597 Maere, T., Verrecht, B., Moerenhout, S., Judd, S., Nopens, I., 2011. BSM-MBR: A  
598 benchmark simulation model to compare control and operational strategies for  
599 membrane bioreactors. *Water Res.* 45, 2181–2190.

600 Mannina, G., Cosenza, A., 2013. The fouling phenomenon in membrane bioreactors:  
601 Assessment of different strategies for energy saving. *J. Memb. Sci.* 444, 332–344.

602 Martin, C., Vanrolleghem, P.A., 2014. Analysing, completing, and generating influent data  
603 for WWTP modelling: A critical review. *Environ. Model. Softw.* 60, 188–201.

604 Moñino, P., Aguado, D., Barat, R., Jiménez, E., Giménez, J.B., Seco, A., Ferrer, J., 2017. A  
605 new strategy to maximize organic matter valorization in municipalities: Combination of  
606 urban wastewater with kitchen food waste and its treatment with AnMBR technology.  
607 *Waste Manag.* 62, 274–289.

608 Moñino, P., Jiménez, E., Barat, R., Aguado, D., Seco, A., Ferrer, J., 2016. Potential use of the  
609 organic fraction of municipal solid waste in anaerobic co-digestion with wastewater in  
610 submerged anaerobic membrane technology. *Waste Manag.* 56, 158–165.

611 Morris, M., 1991. Factorial sampling plans for preliminary computational experiments.  
612 *Technometrics* 33, 239–245.

613 Nguyen, D., Gadhamshetty, V., Nitayavardhana, S., Khanal, S.K., 2015. Automatic process  
614 control in anaerobic digestion technology: A critical review. *Bioresour. Technol.* 193,  
615 513–522.

616 Pianosi, F., Beven, K., Freer, J., Hall, J.W., Rougier, J., Stephenson, D.B., Wagener, T., 2016.  
617 Sensitivity analysis of environmental models: A systematic review with practical  
618 workflow. *Environ. Model. Softw.* 79, 214–232.

619 Pretel, R., Moñino, P., Robles, A., Ruano, M. V., Seco, A., Ferrer, J., 2016. Economic and  
620 environmental sustainability of an AnMBR treating urban wastewater and organic  
621 fraction of municipal solid waste. *J. Environ. Manage.* 179, 83–92.

622 Raskin, L., 2012. Anaerobic membrane bioreactors for sustainable wastewater treatment.  
623 WERF report U4R08.

624 Robles, A., Duran, F., Ruano, M.V., Ribes, J., Rosado, A., Seco, A., Ferrer, J., 2015.  
625 Instrumentation, control, and automation for submerged anaerobic membrane  
626 bioreactors. *Environ. Technol.* 36, 1–12.

627 Robles, A., Ruano, M.V., Ribes, J., Ferrer, J., 2013a. Advanced control system for optimal  
628 filtration in submerged anaerobic MBRs (SAnMBRs). *J. Memb. Sci.* 430, 330–341.

629 Robles, A., Ruano, M. V., Ribes, J., Ferrer, J., 2013b. Factors that affect the permeability of  
630 commercial hollow-fibre membranes in a submerged anaerobic MBR (HF-SAnMBR)  
631 system. *Water Res.* 47, 1277–1288.

632 Robles, A., Ruano, M. V., Ribes, J., Seco, A., Ferrer, J., 2013c. A filtration model applied to

633 submerged anaerobic MBRs (SAnMBRs). *J. Memb. Sci.* 444, 139–147.

634 Robles, A., Ruano, M. V., Ribes, J., Seco, A., Ferrer, J., 2013d. Mathematical modelling of  
635 filtration in submerged anaerobic MBRs (SAnMBRs): Long-term validation. *J. Memb.*  
636 *Sci.* 446, 303–309.

637 Robles, A., Ruano, M. V., Ribes, J., Seco, A., Ferrer, J., 2014a. Model-based automatic tuning  
638 of a filtration control system for submerged anaerobic membrane bioreactors (AnMBR).  
639 *J. Memb. Sci.* 465, 14–26.

640 Robles, A., Ruano, M. V., Ribes, J., Seco, A., Ferrer, J., 2014b. Global sensitivity analysis of  
641 a filtration model for submerged anaerobic membrane bioreactors (AnMBR). *Bioresour.*  
642 *Technol.* 158, 365–373.

643 Saltelli, A., Chan, K., Scott, E.M., 2000. *Sensitivity Analysis*. John Wiley & Sons, New York.

644 Sheets, J.P., Yang, L., Ge, X., Wang, Z., Li, Y., 2015. Beyond land application: Emerging  
645 technologies for the treatment and reuse of anaerobically digested agricultural and food  
646 waste. *Waste Manag.* 44, 94–115.

647 Verrecht, B., Maere, T., Nopens, I., Brepols, C., Judd, S., 2010. The cost of a large-scale  
648 hollow fibre MBR. *Water Res.* 44, 5274–5283.

649 Yang, M., Wei, Y., Zheng, X., Wang, F., Yuan, X., Liu, J., Luo, N., Xu, R., Yu, D., Fan, Y.,  
650 2016. CFD simulation and optimization of membrane scouring and nitrogen removal for  
651 an airlift external circulation membrane bioreactor. *Bioresour. Technol.* 219, 566–575.

652 Yang, M., Yu, D., Liu, M., Zheng, L., Zheng, X., Wei, Y., Wang, F., Fan, Y., 2017.  
653 Optimization of MBR hydrodynamics for cake layer fouling control through CFD  
654 simulation and RSM design. *Bioresour. Technol.* 227, 102–111.

655

656 **Figure captions**

657 **Figure 1.** (A) Sequence of the different operational stages in the membrane modules during  
658 the alternative operating mode and (B) flow diagram of the proposed optimization  
659 methodology

660 **Figure 2.** (A) Values of BRF and SRF and (B)  $t_F$  and  $t_{BF}$  optimized by the supervisory  
661 controller. The results were obtained using UWW as substrate

662 **Figure 3.** Evolution of the TMPs and different stages simulated. The results were obtained  
663 using UWW as substrate

664 **Figure 4.** (A) Values of BRF and SRF and (B)  $t_F$  and  $t_{BF}$  optimized by the supervisory  
665 controller. The results were obtained using UWW and FW as substrates

666 **Figure 5.** Evolution of the energy requirements of the filtration process with the controller  
667 operating at  $17 \text{ g}\cdot\text{l}^{-1}$  MLTS entering the membrane tanks. The results for feeding strategies are  
668 shown: (A) UWW and (B) mixture of UWW and FW

669 **Figure 6.** Evolution of the costs of the filtration process with the controller operating at  $17 \text{ g}\cdot\text{l}^{-1}$   
670 MLTS entering the membrane tanks. The results for feeding strategies are shown: (A) UWW  
671 and (B) mixture of UWW and FW

672 **Table captions**

673 **Table 1.** Average values of the operational parameters evaluated in this study. The intervals  
674 of uncertainty, as well as the initial values for the model-based supervisory controller (Monte  
675 Carlo results) are also presented

676 **Table 2.** Sensitivity rankings for  $r_{opt}$  with UWW as substrate ( $r_{opt} = 60$ ) and the mixture of  
677 UWW and FW ( $r_{opt} = 40$ )

678 **Table 3.** Average energy requirements of the filtration process with the controller operating at  
679  $17 \text{ g}\cdot\text{l}^{-1}$  MLTS entering the membrane tanks

680 **Table 4.** Average costs of the filtration process with the controller operating at  $17 \text{ g}\cdot\text{l}^{-1}$  MLTS  
681 entering the membrane tanks



682 **Supplementary material**

683 **Figure S1.** Net transmembrane flow ( $J_{\text{net}}$ ) applied during the validation of the supervisory  
684 controller by simulation. The corresponding values of the MLTS concentrations in the  
685 membrane tanks ( $\text{MLTS}_{\text{MT}}$ ) during the co-digestion experiment at  $17 \text{ g}\cdot\text{l}^{-1}$  are also shown

686 **Figure S2.** TMP simulated by the model ( $\text{TMP}_{\text{sim}}$ ) vs experimental TMP ( $\text{TMP}_{\text{exp}}$ )

687 Hierarchical clustering analysis based on the absolute means of the selected parameters with  
688 UWW as substrate

689 **Figure S3.** Hierarchical clustering analysis based on the absolute means of the selected  
690 parameters obtained (A) with (a) UWW as substrate and (B) with UWW and FW as substrates

691 **Figure S4.** Sensitivity measurements ( $\mu^*$  and  $\sigma$ ) obtained (A) with UWW as substrate ( $r_{\text{opt}}$  of  
692 60) and (B) with the mixture of UWW and FW as substrate ( $r_{\text{opt}}$  of 40)

693 **Figure S5.** Correlation matrix ( $\alpha = 0.05$ ;  $n = 999$ ) of the optimized parameters, the energy  
694 requirements and the filtration costs obtained (A) with UWW as substrate and (B) with  
695 mixture of UWW and FW as substrate. The  $\text{MLTS}_{\text{MT}}$ ,  $J_{\text{net}}$  and TMP are also included

696

697

698

699

700

701

702

703

704

705

706

- 707 **Abbreviation and symbols**
- 708 **AeMBR** - Aerobic membrane bioreactor
- 709 **AnMBR** - Submerged anaerobic membrane bioreactor
- 710 **BRF** – Biogas recycling flow-rate
- 711 **BF** – Back-flushing period
- 712 **C<sub>B</sub>** – Operating cost of membrane scouring by biogas sparging
- 713 **C<sub>LIFESPAN</sub>** – Cost of membrane replacement due to irreversible fouling.
- 714 **C<sub>REAGENTS</sub>** – Cost of reagents needed to clean irreversible fouling
- 715 **C<sub>SRF</sub>** – Operating cost of pumping the sludge
- 716 **C<sub>STAGE</sub>** – Operating cost of pumping permeate
- 717 **CT** – Control time
- 718 **C<sub>TOTAL</sub>** – Total operating costs
- 719 **C<sub>W</sub>** – Total energetic cost
- 720 **D** – Pipe diameter
- 721 **E<sub>COST</sub>** – Cost of energy
- 722 **EE<sub>i</sub>** – Elemental effects of each input factor on the model output
- 723 **f** – Number of filtration periods
- 724 **fr** – Friction factor
- 725 **F** – Filtration period
- 726 **f<sub>BF</sub>** – Back-flush frequency
- 727 **F<sub>i</sub>** – Scaled elementary effect distribution
- 728 **g** – Acceleration of gravity
- 729 **GSA** – Global sensitivity analysis
- 730 **HCA** – Hierarchical clustering analysis
- 731 **HRT** – Hydraulic retention time

- 732  **$J_{BF}$**  – Transmembrane flow during back-flush
- 733  **$J_{net}$**  – Net transmembrane flow
- 734  **$L$**  – Pipe length
- 735  **$L_{eq}$**  – Equivalent pipe length of accidental pressure drops
- 736  **$M$**  – Molar flow rate of biogas
- 737 **MBR** - Membrane bioreactor
- 738 **MLTS** – Mixed liquor total solids
- 739  **$MLTS_{MT}$**  – MLTS concentration in the membrane tanks
- 740 **OFMSW** - Organic fraction of municipal solid waste
- 741  **$P_1$**  – Absolute inlet pressure
- 742  **$P_2$**  – Absolute outlet pressure
- 743  **$q$**  – Volumetric flow rate
- 744  **$R$**  – Relaxation period
- 745  **$R_g$**  – Ideal gas constant
- 746  **$R_C$**  – Resistance of the solid cake formed on the surface of the membrane
- 747  **$R_I$**  – Resistance due to irreversible fouling of the membrane
- 748  **$R_M$**  – Resistance intrinsic to the membrane
- 749  **$r_{opt}$**  – Optimum number of times that the  $SEE_i$  should be calculated
- 750  **$R_T$**  – Total filtration resistance
- 751  **$SEE_i$**  – Scaled elementary effect
- 752  **$SDG_m$**  – Specific demand of gas per square meter of membrane
- 753 **SRF** – Sludge recycling flow-rate
- 754 **SRT** – Solids retention time
- 755  **$t_{BF}$**  – Duration of the back-flushing stage
- 756  **$t_F$**  – Duration of the filtration stage

- 757  $T_{\text{gas}}$  – Biogas temperature
- 758  $\text{TMP}$  – Transmembrane pressure
- 759  $\text{TMP}_{\text{sim}}$  – Simulated transmembrane pressure
- 760  $\text{TMP}_{\text{exp}}$  – Experimental transmembrane pressure
- 761  $\text{TS}$  – Total solids
- 762  $t_{\text{R}}$  – Duration of the relaxation stage
- 763  $\text{UWW}$  - Urban wastewater
- 764  $\mathbf{V}$  – Fluid velocity
- 765  $\mathbf{V}_{\text{T}}$  – Net volume of treated wastewater
- 766  $\mathbf{W}_{\text{back-flushing}}$  – Energy requirements of the back-flushing pump
- 767  $\mathbf{W}_{\text{BRF}}$  – Energy requirements of the biogas lower
- 768  $\mathbf{W}_{\text{filtration}}$  – Energy requirements of the permeate filtration pump
- 769  $\mathbf{W}_{\text{SRF}}$  – Energy requirements of the sludge recycling pump
- 770  $\mathbf{X}_{\text{mC}}$  – Dry mass of cake in the membrane surface
- 771  $\mathbf{X}_{\text{mI}}$  – Dry mass of irreversible fouling on the membrane surface
- 772  $\mathbf{X}_{\text{TS}}$  – Concentration of total solids in the mixed liquor
- 773  $\mathbf{Z}_1\text{-}\mathbf{Z}_2$  – difference in height
- 774  $\alpha$  – Compression index
- 775  $\alpha_{\text{C}}$  – Average specific resistance of the solid cake
- 776  $\alpha_{\text{I}}$  – Average specific resistance of the irreversible fouling
- 777  $\sigma$  – Standard deviation
- 778  $\rho_{\text{sludge}}$  – sludge density
- 779  $\eta_{\text{blower}}$  – Overall mechanical and electrical efficiency of the blower
- 780  $\eta_{\text{pump}}$  – Overall mechanical and electrical efficiency of the pump
- 781  $\mu$  – Mean

- 782  $\mu^*$  – Absolute mean ( $\mu^*$ )
- 783  $\mu_p$  – Dynamic viscosity of the permeate
- 784  $\omega_C$  – Mass of solids settled per membrane area
- 785  $\omega_I$  – Mass of irreversible fouling per membrane area
- 786  $\Delta R_{I,MAX}$  – Upper threshold of irreversible fouling resistance at which membrane cleaning
- 787 starts
- 788

## Graphical abstract

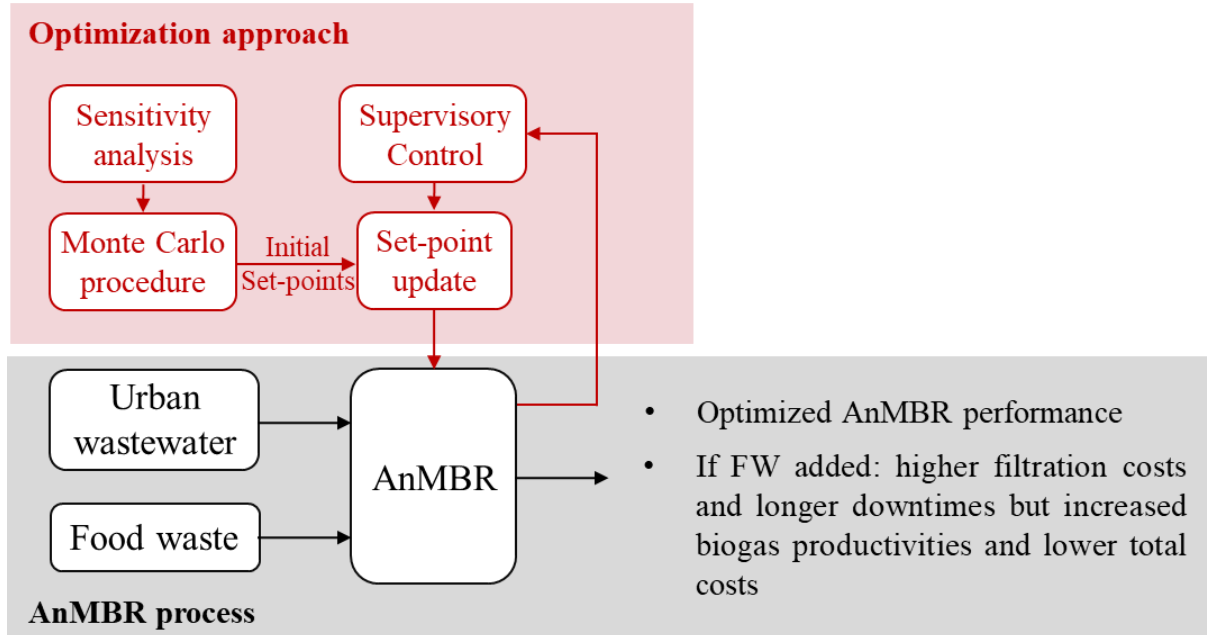


**Table 1.** Average values of the operational parameters evaluated in this study. The intervals of uncertainty, as well as the initial values for the model-based supervisory controller (Monte Carlo results) are also presented

| Parameter | Units                            | Substrate | Average values | Minimum | Maximum | Monte Carlo results |
|-----------|----------------------------------|-----------|----------------|---------|---------|---------------------|
| BRF       | $\text{m}^3 \cdot \text{h}^{-1}$ | UWW       | 12             | 3       | 21      | 13                  |
|           |                                  | UWW +FW   | 12             | 3       | 21      | 13                  |
| SRF       | $\text{m}^3 \cdot \text{h}^{-1}$ | UWW       | 2.1            | 1.5     | 2.7     | 2.0                 |
|           |                                  | UWW +FW   | 2.1            | 1.5     | 2.7     | 1.8                 |
| $t_F$     | s                                | UWW       | 400            | 200     | 600     | 600                 |
|           |                                  | UWW +FW   | 400            | 200     | 600     | 485                 |
| $t_R$     | s                                | UWW       | 35             | 10      | 60      | 10                  |
|           |                                  | UWW +FW   | 35             | 10      | 60      | 10                  |
| $t_{BF}$  | s                                | UWW       | 35             | 10      | 60      | 17                  |
|           |                                  | UWW +FW   | 35             | 10      | 60      | 31                  |
| $f_{BF}$  | -                                | UWW       | 11             | 1       | 21      | 10                  |
|           |                                  | UWW +FW   | 11             | 1       | 21      | 4                   |
| $J_{BF}$  | LMH                              | UWW       | 15             | 10      | 20      | 16                  |
|           |                                  | UWW +FW   | 15             | 10      | 20      | 10                  |

**Table 2.** Sensitivity rankings for  $r_{\text{opt}}$  with UWW as substrate ( $r_{\text{opt}} = 60$ ) and the mixture of UWW and FW ( $r_{\text{opt}} = 40$ )

| UWW                   |         |          | UWW + FW              |         |          |
|-----------------------|---------|----------|-----------------------|---------|----------|
| Parameter             | $\mu^*$ | $\sigma$ | Parameter             | $\mu^*$ | $\sigma$ |
| <b>BRF</b>            | 1.253   | 1.856    | <b>BRF</b>            | 1.355   | 2.099    |
| <b>f<sub>BF</sub></b> | 0.770   | 2.220    | <b>f<sub>BF</sub></b> | 0.579   | 1.418    |
| <b>t<sub>F</sub></b>  | 0.724   | 1.921    | <b>t<sub>BF</sub></b> | 0.344   | 1.059    |
| <b>t<sub>BF</sub></b> | 0.574   | 1.210    | <b>t<sub>F</sub></b>  | 0.252   | 0.710    |
| <b>SRF</b>            | 0.464   | 1.584    | <b>SRF</b>            | 0.163   | 0.410    |
| <b>t<sub>R</sub></b>  | 0.057   | 0.261    | <b>t<sub>R</sub></b>  | 0.067   | 0.138    |
| <b>J<sub>BF</sub></b> | 0.057   | 0.268    | <b>J<sub>BF</sub></b> | 0.005   | 0.018    |



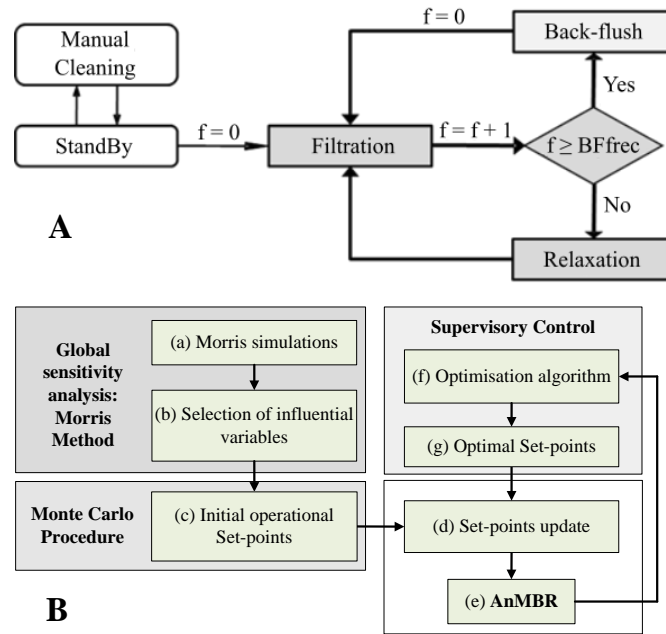
**Table 3.** Average energy requirements of the filtration process with the controller operating at 17 g·l<sup>-1</sup> MLTS entering the membrane tanks

| Substrate | $W_{\text{TOTAL}}$ (kWh·m <sup>-3</sup> ) | $W_{\text{BRF}}$ (%) | $W_{\text{SRF}}$ (%) | $W_{\text{Stage}}$ (%) |
|-----------|---|----------------------|----------------------|------------------------|
| UWW       | 0.20                                      | 79.7                 | 16.9                 | 14.3                   |
| UWW + FW  | 0.34                                      | 88.5                 | 9.6                  | 9.8                    |

**Table 4.** Average costs of the filtration process with the controller operating at  $17 \text{ g}\cdot\text{l}^{-1}$  MLTS entering the membrane tanks

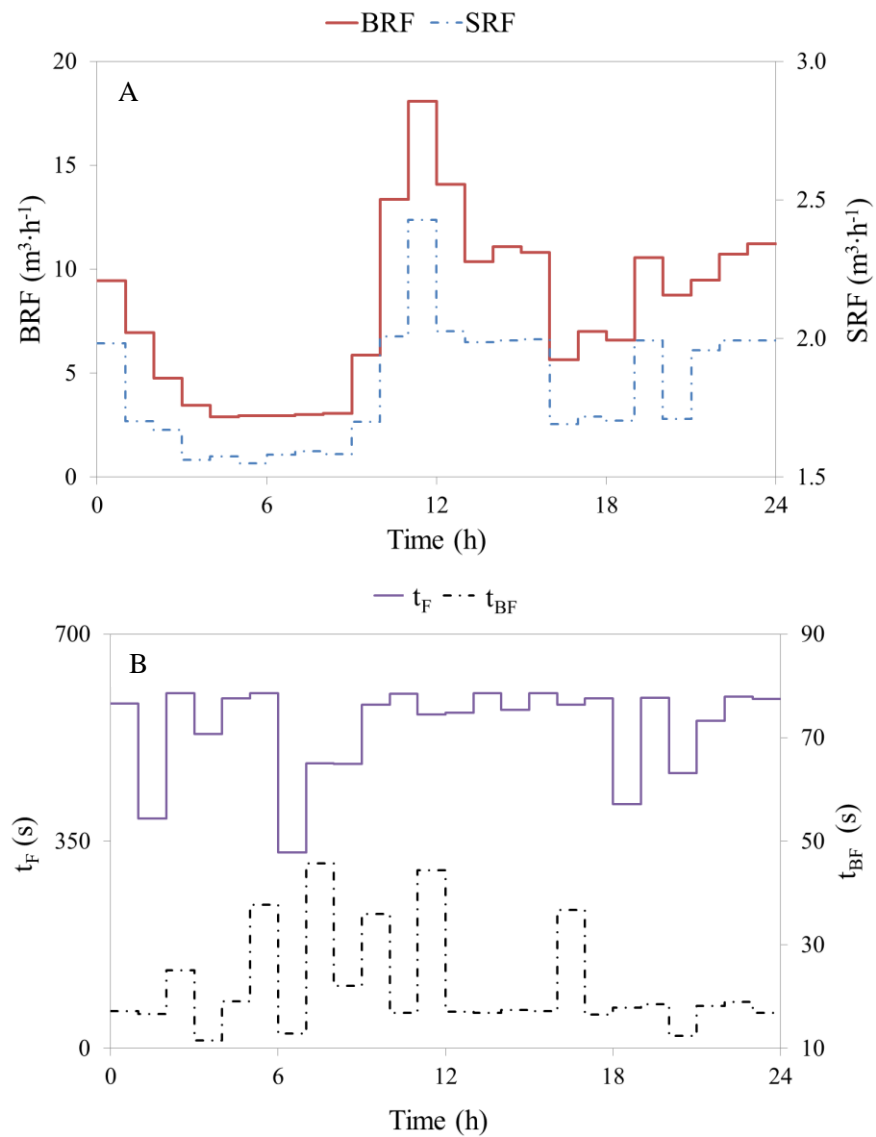
| <b>Substrate</b> | <b>C<sub>TOTAL</sub> (€ per m<sup>3</sup>)</b> | <b>C<sub>W</sub> (%)</b> | <b>C<sub>REAGENTS</sub> (%)</b> | <b>C<sub>LIFESPAN</sub> (%)</b> |
|------------------|--|--------------------------|---------------------------------|---------------------------------|
| <b>UWW</b>       | 0.047  | 59.6                     | 17.0                            | 23.4                            |
| <b>UWW + FW</b>  | 0.067  | 69.0                     | 13.0                            | 18.0                            |

Figure 1



**Figure 1.** (A) Sequence of the different operational stages in the membrane modules during the alternative operating mode and (B) flow diagram of the proposed optimization methodology

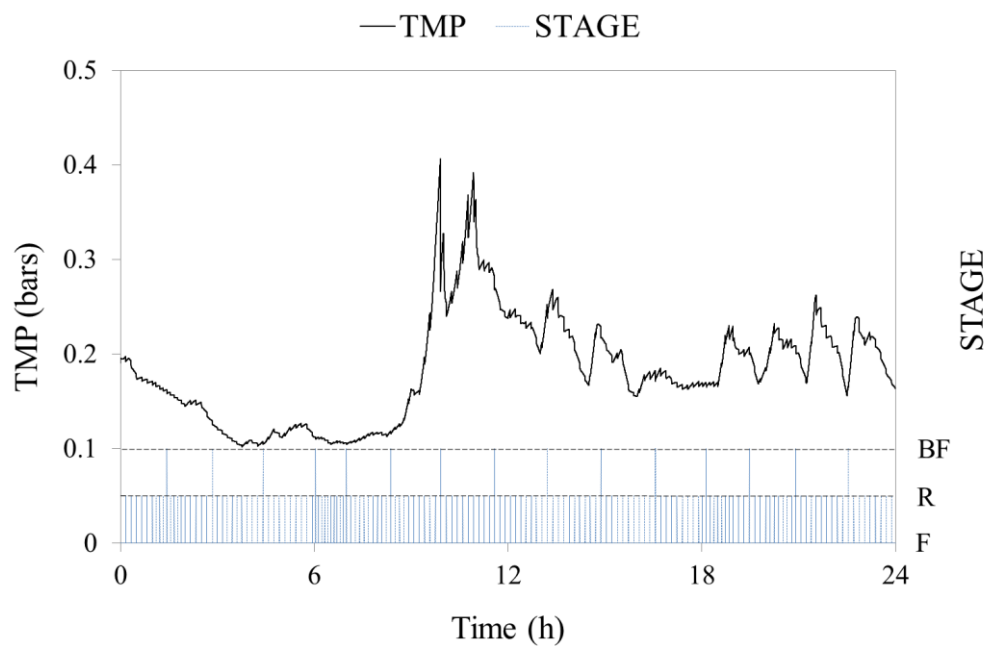
Figure 2



**Figure 2.** (A) Values of BRF and SRF and (B)  $t_F$  and  $t_{BF}$  optimized by the supervisory controller.

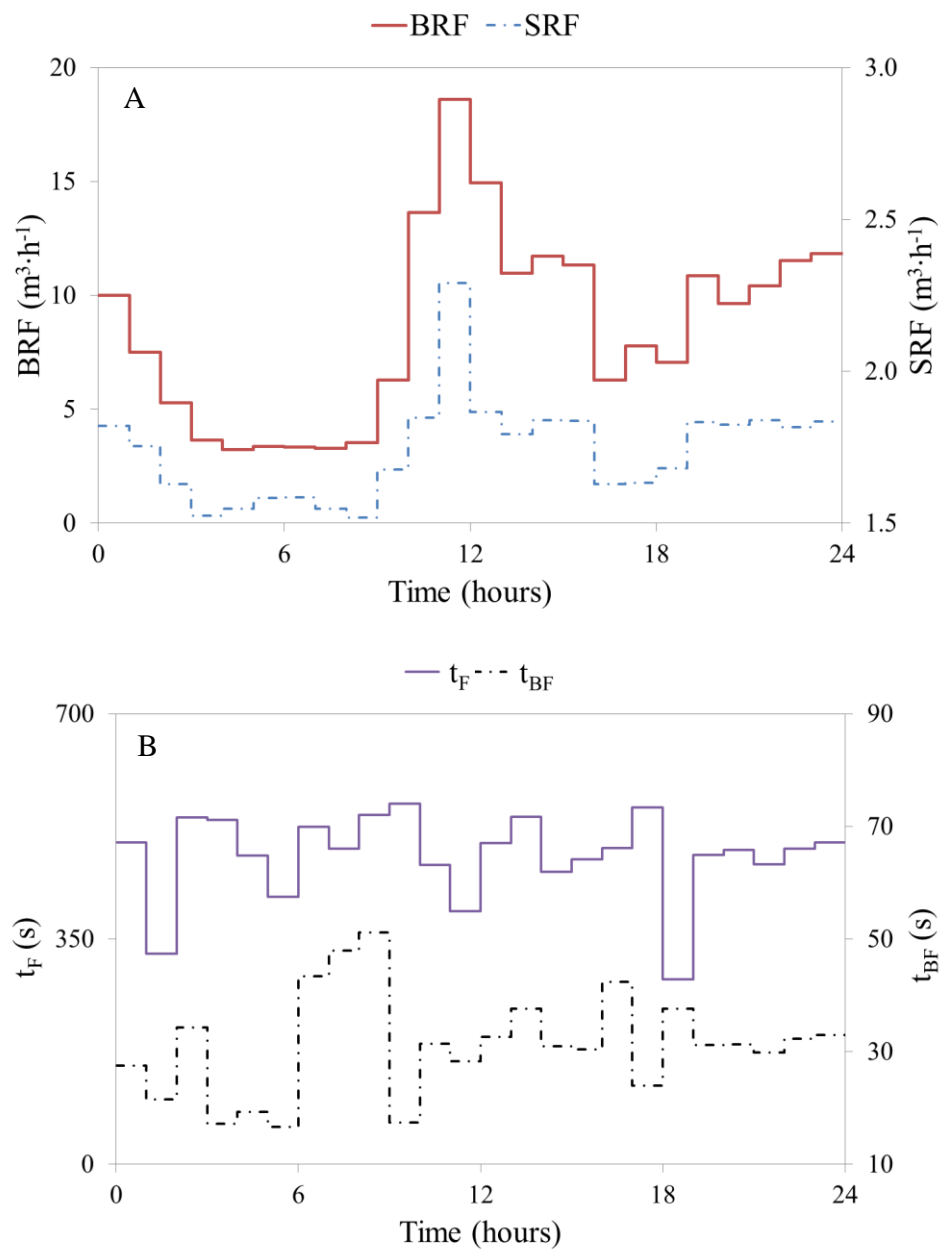
The results were obtained by applying the transmembrane flux shown in Figure S1 with a MLTS concentration entering the tanks of  $17 \text{ g} \cdot \text{l}^{-1}$  and using UWW as substrate

**Figure 3**



**Figure 3.** Evolution of the TMPs and different stages simulated. The results were obtained by applying the transmembrane flux shown in Figure S1 with a MLTS concentration entering the tanks of  $17 \text{ g}\cdot\text{l}^{-1}$  and using UWW as substrate

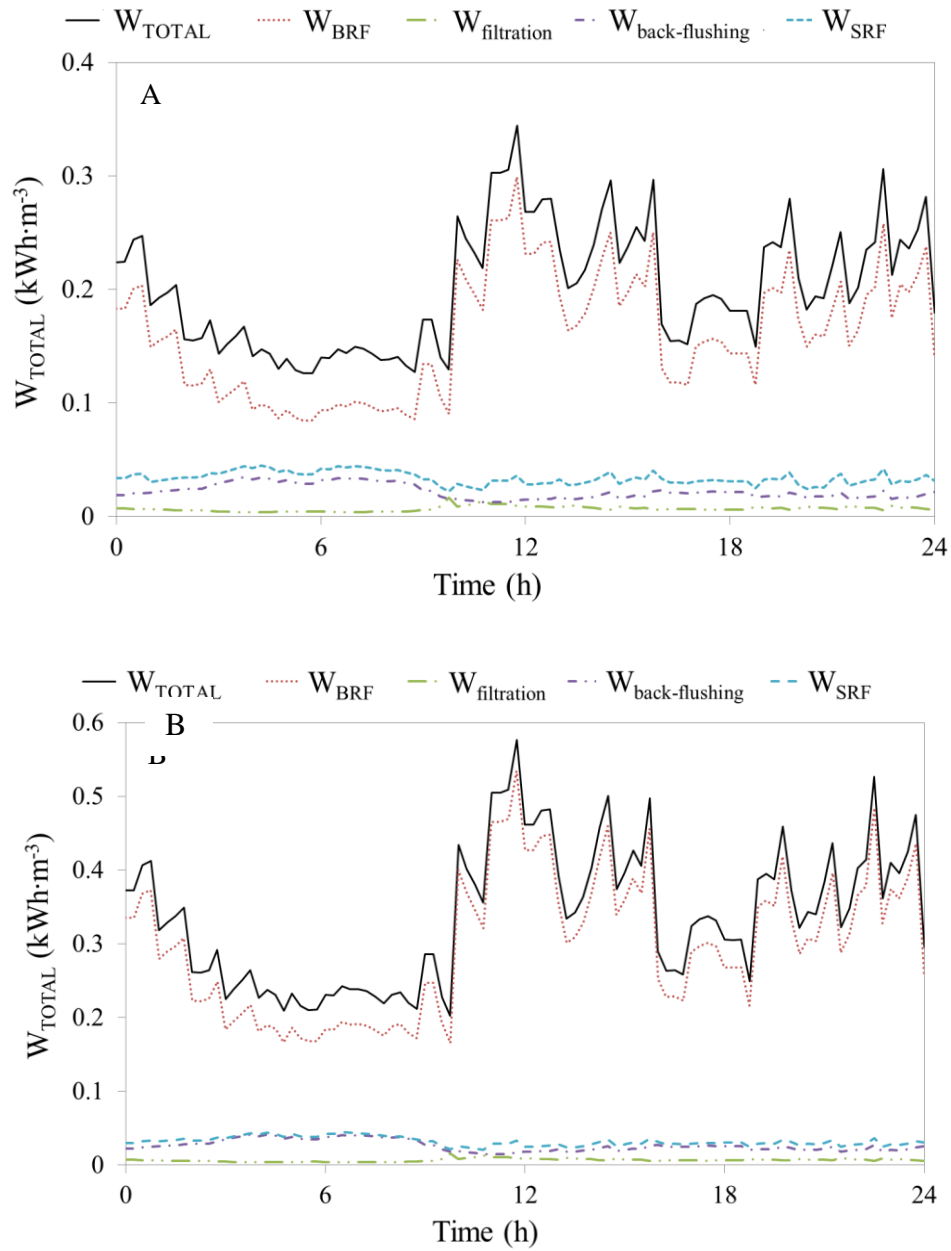
Figure 4



**Figure 4.** (A) Values of BRF and SRF and (B)  $t_F$  and  $t_{BF}$  optimized by the supervisory controller.

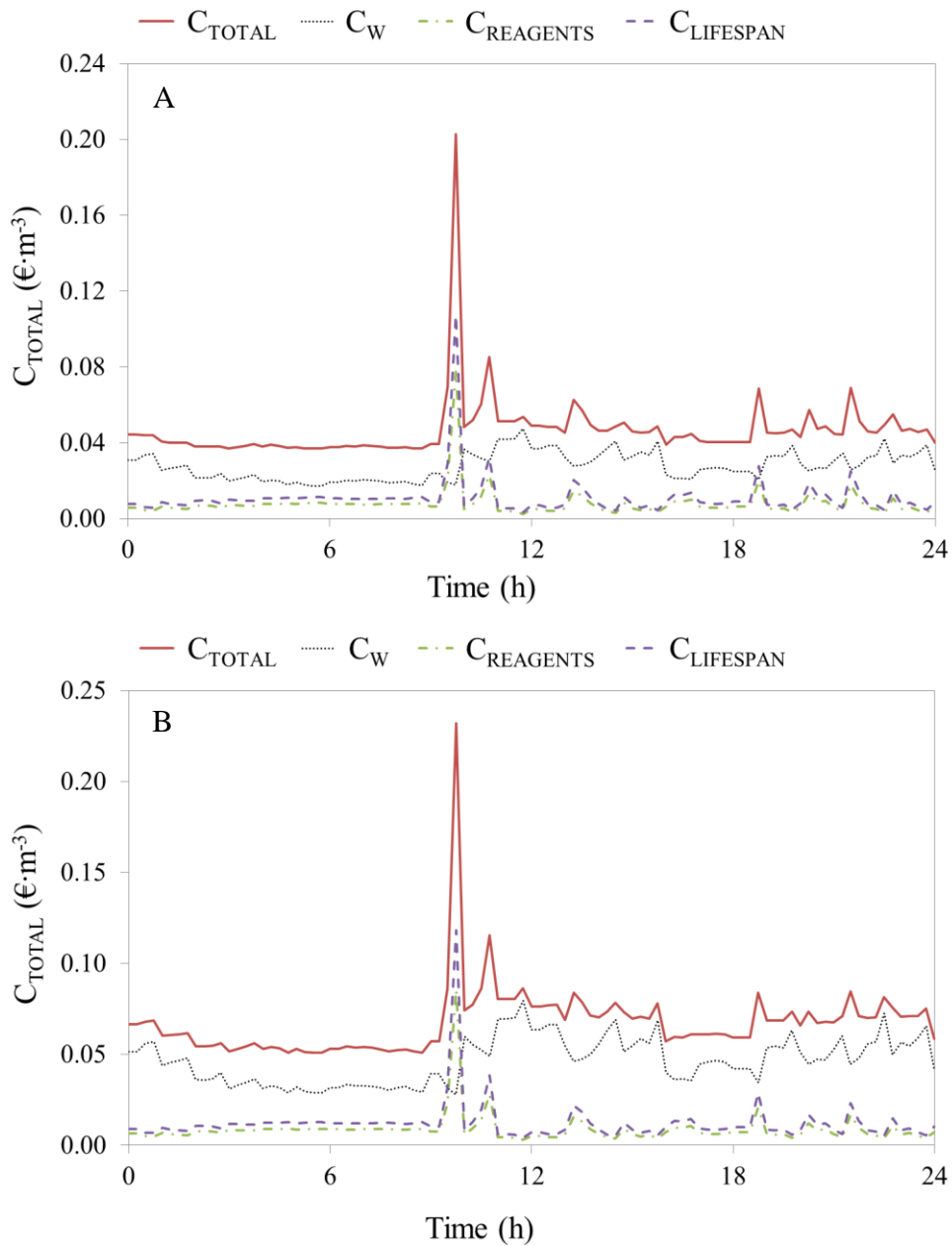
The results were obtained by applying the transmembrane flux shown in Figure S1 with a MLTS concentration entering the tanks of 17 g·l<sup>-1</sup> and using UWW and FW as substrates

Figure 5



**Figure 5.** Evolution of the energy requirements of the filtration process with the controller operating at 17 g·l<sup>-1</sup> MLTS entering the membrane tanks. The results for feeding strategies are shown: (A) UWW and (B) mixture of UWW and FW

Figure 6



**Figure 6.** Evolution of the costs of the filtration process with the controller operating at  $17 \text{ g}\cdot\text{l}^{-1}$  MLTS entering the membrane tanks. The results for feeding strategies are shown: (A) UWW and (B) mixture of UWW and FW



**E-Component 1**

[Click here to download E-Component: Figure S1.docx](#)

**E-Component 2**

[Click here to download E-Component: Figure S2.docx](#)

### E-Component 3

[Click here to download E-Component: Figure S3.docx](#)

**E-Component 4**

[Click here to download E-Component: Figure S4.docx](#)

## E-Component 5

[Click here to download E-Component: Figure S5.docx](#)